

UC Davis

UC Davis Previously Published Works

Title

Auricle shaping using 3D printing and autologous diced cartilage

Permalink

<https://escholarship.org/uc/item/7hw019n7>

Journal

The Laryngoscope, 129(11)

ISSN

0023-852X

Authors

Liao, Junlin
Chen, Yong
Chen, Jia
et al.

Publication Date


2019-11-01

DOI

10.1002/lary.27752

Peer reviewed

Auricle Shaping Using 3D Printing and Autologous Diced Cartilage

Junlin Liao, MD ; Yong Chen, MD; Jia Chen; Bin He; Li Qian; Jiaqin Xu; Aijun Wang, PhD;
Qingfeng Li, MD; Hongju Xie; Jianda Zhou, MD

Objective: To reconstruct the auricle using a porous, hollow, three-dimensional (3D)-printed mold and autologous diced cartilage mixed with platelet-rich plasma (PRP).

Methods: Materialise Magics v20.03 was used to design a 3D, porous, hollow auricle mold. Ten molds were printed by selective laser sintering with polyamide. Cartilage grafts were harvested from one ear of a New Zealand rabbit, and PRP was prepared using 10 mL of auricular blood from the same animal. Ear cartilage was diced into 0.5- to 2.0-mm pieces, weighed, mixed with PRP, and then placed inside the hollow mold. Composite grafts were then implanted into the backs of respective rabbits (n = 10) for 4 months. The shape and composition of the diced cartilage were assessed histologically, and biomechanical testing was used to determine stiffness.

Results: The 3D-printed auricle molds were 0.6-mm thick and showed connectivity between the internal and external surfaces, with round pores of 0.1 to 0.3 cm. After 4 months, the diced cartilage pieces had fused into an auricular shape with high fidelity to the anthropotomy. The weight of the diced cartilage was 5.157 ± 0.230 g ($P > 0.05$, compared with preoperative). Histological staining showed high chondrocyte viability and the production of collagen II, glycosaminoglycans, and other cartilaginous matrix components. In unrestricted compression tests, auricle stiffness was 0.158 ± 0.187 N/mm, similar to that in humans.

Conclusion: Auricle grafts were constructed successfully through packing a 3D-printed, porous, hollow auricle mold with diced cartilage mixed with PRP. The auricle cartilage contained viable chondrocytes, appropriate extracellular matrix components, and good mechanical properties.

Key Words: Diced cartilage, platelet-rich plasma, 3D printing, porous hollow mold, auricle, reconstruction.

Levels of Evidence: NA.

Laryngoscope, 129:2467–2474, 2019

INTRODUCTION

External ear reconstruction for congenital microtia remains a surgical challenge and a controversial issue. A successful auricle reconstruction must include the complex three-dimensional (3D) contour of the external ear, its biomechanical features, and considerable flexibility. The current

methods of reconstruction typically use autologous costal cartilage grafts, prosthetic reconstruction, or polymer implants, such as Medpor (Porex Surgical Inc., Newnan, US).^{1–4} However, it is very difficult to meet the functional requirements, shape fidelity, and flexibility through any one approach. For example, carved costal cartilage retains a certain level of compliance but lacks the required flexibility, and it has somewhat unpredictable cosmetic results because it is difficult for plastic surgeons to sculpt a scaffold that completely and anatomically matches the normal ear. The use of costal cartilage autografts has the added risk of hemopneumothorax and an incomplete chest wall postoperatively.

To create an elastic ear cartilage bearing the necessary complex biomechanical properties and morphological characteristics, a plastic surgeon needs to have good sculpting skills and 3D awareness.^{5–8} Medpor (Stryker) is a synthetic porous implant, and its use eliminated the additional morbidity associated with harvesting autologous rib cartilage. However, the Medpor constructs are inflexible, and this runs the long-term risk of extrusion through the skin.⁹ In recent years, the emergence of tissue engineering has provided a new avenue for the repair of tissue defects. Cartilage tissue engineering offers the potential to create a more anatomically accurate auricle for external ear reconstruction.^{8,10} However, one of the main obstacles with ear tissue engineering is that ear cartilage in vivo is unable to keep its original size and shape.^{8,11} In addition, there are insufficient seed cells to proliferate and completely replace the scaffold,¹² and biomechanical strength of the cultivated auricle cannot

This is an open access article under the terms of the Creative Commons Attribution-NonCommercial License, which permits use, distribution and reproduction in any medium, provided the original work is properly cited and is not used for commercial purposes.

From the Departments of Medical Cosmetology, The First Affiliated Hospital, University of South China (J.L., H.X.), Hengyang; the Departments of Plastic and Reconstructive Surgery, The Third Xiangya Hospital, Central South University (J.L., Y.C., J.C., B.H., J.X., J.Z.); the Emergency Department, The First Hospital of Changsha (Y.C.); the Departments of Burn and Plastic Surgery, The Second Xiangya Hospital, Central South University (L.Q.), Changsha; the Departments of Burn and Plastic Surgery, Ningxiang People's Hospital (B.H.), Ningxiang, Hunan; the Departments of Burn and Plastic Surgery, Hainan People's Hospital (J.X.), Haikou, Hainan; the Department of Plastic and Reconstructive Surgery, Shanghai Jiaotong University Medical School, Ninth People's Hospital (Q.L.), Shanghai, People's Republic of China; and the Department of Surgery, Davis Health System, University of California (A.W.), Sacramento, California, U.S.A.

Editor's Note: This Manuscript was accepted for publication on November 19, 2018.

The authors have no funding, financial relationships, or conflicts of interest to disclose.

Send correspondence to Prof. Jianda Zhou, Departments of Plastic and Reconstructive Surgery, The Third Xiangya Hospital, Central South University, Changsha, Hunan, 410013, People's Republic of China. E-Mail: doctorzhoujianda@163.com and Prof. Hongju Xie, Departments of Medical Cosmetology, The First Affiliated Hospital, University of South China, Chuan-shan Road, Hengyang, Hunan, 421001, China. E-Mail: 2553158@qq.com

DOI: 10.1002/lary.27752

withstand the normal levels of contraction of the skin *in vivo*.^{13,14}

Diced cartilage grafts are increasingly used in rhinoplasty and achieve good aesthetic results.¹⁵ However, a diced cartilage graft is unable to provide strong support or maintain a specific shape. For this reason, few studies have tested the use of diced cartilage grafts in ear reconstruction. An inherent advantage of diced cartilage is that it is very easy to mold to any shape. In our preliminary studies, we found that fused diced cartilage has good mechanical strength and flexibility. In addition, we found that mixing the cartilage with a platelet-rich plasma (PRP) improved the viability of the diced cartilage when wrapped in a poly(lactic-co-glycolic acid) (PLGA) membrane.^{16,17} However, whether diced cartilage can be used to reconstruct an ear-shaped hollow framework for ear reconstruction is unknown.

Three-dimensional printing technology has been widely used in the biomedical field for tissue engineering and regenerative medicine.¹⁸ Compared with traditional processes of scaffold fabrication, such as gas foaming, solvent casting, freeze drying, and electrostatic spinning, 3D printing has obvious advantages, with the ability to control the production of a 3D porous and complex internal structure for the adhesion and proliferation of cells. More importantly, its shape can be anatomically matched to the structure of defective tissues.¹⁹

The purpose of this study was to explore the potential applications of an image-based computer-aided design (CAD) and 3D-printed porous hollow auricle mold filled with diced cartilage and PRP for auricular reconstruction. Referring to the principles of tissue engineering, the diced cartilage would provide the seed cells; PRP would provide the necessary growth factors; and the porous hollow scaffold would provide an appropriate scaffold for cell attachment and growth.

MATERIALS AND METHODS

Ten New Zealand white rabbits were acquired for this study. They were 4 months old and weighed 2.50 to 2.90 kg. This study was approved by the Laboratory Animal Management and Ethics Committee of the Third Xiangya Hospital of Central South University (Changsha, Hunan, People's Republic of China). All procedures complied with the Laboratory Animal Administration Rules of China.

Design and Fabrication of the Porous Hollow Mold

A porous, hollow, auricle-shaped mold required the following characteristics: 1) a 3D appearance; 2) a hollow inside for packing diced cartilage; 3) a porous surface, with pores of various sizes to facilitate nutrient delivery, exchange of metabolic waste, and ingrowth of capillaries; 4) be prepared from a biocompatible material to reduce rejection and allow the diced cartilage to mold to the auricle shape gradually; 5) be cost-effective; and 6) be reproducible and utilize easily accessible material.

Skull 3D computed tomographic imaging data (Digital Communications and Communications in Medicine data) of a patient with microtia were collected, and slice images of a reference auricle were obtained and adapted to an ear-shaped mold model as Stereolithography (STL) files using Materialise Magics v20.03 (Materialise, Leuven, Belgium). Contours and key landmarks, such as the helix, antihelix, tragus, antitragus, fossa triangularis, and lobule, were accentuated to ensure that the features remained defined when filled with diced cartilage. The size of the hollow porous mold was modified to the 3/5 size of a normal auricle to accommodate the ear cartilage (Fig. 1). The resulting model was printed in 3D using a selective laser sintering (SLS) printer (Huashu, Inc., Hunan, China) with polyamide (Huashu, Inc., Hunan, China).

In preliminary experiments, a different prototype was designed and printed, with pores of 0.3 to 0.5 cm in size that were randomly distributed on the surface. However, these bigger-diameter pores led to leakage of the diced cartilage pieces.

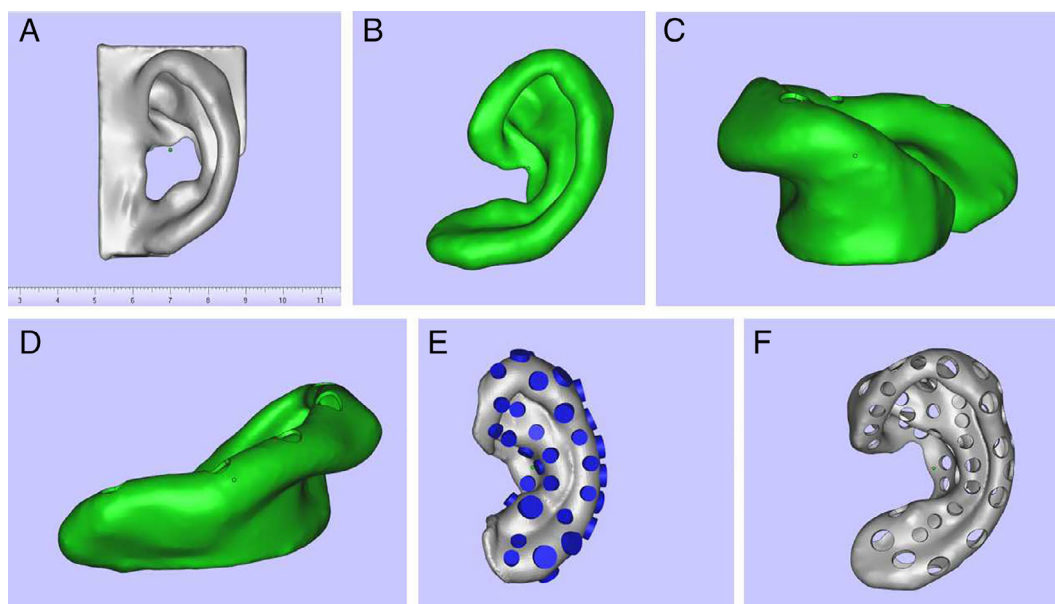


Fig. 1. Design of the porous, hollow auricle mold. (A) Solid model. (B–D) Front and side views after base removal. (E) Design of the pores on the surface. (F) View after completion of model design. [Color figure can be viewed in the online issue, which is available at www.laryngoscope.com.]

We therefore designed a mold with smaller pores that would facilitate angiogenesis, nutrient, and gas exchange without the loss of cartilage pieces.

Preparation of Platelet-Rich Plasma

Platelet-rich plasma was prepared during the surgical procedure, as described previously.²⁰ Briefly, 10 mL of blood from each animal was mixed with 3.8% sodium citrate to prevent coagulation. This resulted in a red and opaque lower fraction consisting of red and white blood cells and platelets, called the *blood cell component*, and an upper yellow turbid fraction containing plasma and platelets, called the *serum component*. The entire serum component and upper 6 to 8 mm of the blood cell component were transferred into a sterile Vacurette (Olympus, Center Valley PA) without citrate and centrifuged at $1,228 \times g$ for 5 minutes. The top serum component was removed, and the remaining fraction was retained as the concentrated platelets, that is, as PRP.

In Vivo Implantation and Harvesting

Each rabbit was subjected to general anesthesia by an intramuscular injection of 2% xylazine hydrochloride at 0.05 mL/kg and an intravenous injection of 3% pentobarbital sodium at 0.5 mL/kg into the ear. Local anesthesia was induced by 0.5% lidocaine. Cartilage grafts were harvested from one ear. The perichondrium was removed, and the auricle cartilage was cut into approximately 0.5- to 2.0-mm pieces and weighed. The size of cartilage fragments used in the experiment is 0.5- to 2.0-mm, and the size difference is relatively large. However, it does not influence the diced cartilages fused into a whole in our preliminary studies.^{16,17} The sedated rabbit was then shaved across the back and the operative site cleaned with depilatory paste. The skin was prepared with a povidone/iodine solution and draped in a sterile fashion with a disposable towel. A 3- to 4-cm linear skin incision was made, and a subcutaneous skin pocket was created. Diced

cartilages were mixed with PRP and placed into the mold, completely filling the mold. The graft was then inserted inside the skin pocket. A 10-mL syringe was used to apply negative pressure. The skin was closed with a 4/0 polyglactin sutures (Fig. 2). To prevent infection, a single intramuscular injection of 50 mg/kg ceftriaxone was administered.

Sample Collection

Animals were maintained for 4 months and then euthanized. No complications (e.g., hematoma, seroma, or infection) were observed at the implantation site during the postoperative period. The rabbits were anesthetized, and the implants were dissected for gross observation and biomechanical assessments. Hematoxylin and eosin (HE), safranin O, Masson's trichrome, toluidine blue, and type II collagen immunohistochemical staining were performed to comprehensively evaluate the viability of cartilage, extracellular matrix components, and the production of type II collagen.

Unconfined Compression Test

The newly formed auricles were subjected to whole-ear, helix-down, unconfined compression testing to determine whole-ear stiffness. Compression platens were used to load at a constant displacement rate of 10 mm/min. A preload of ~4.5 grams was applied to define the start of the test and to maintain the specimen in the helix-down position. Stiffness was calculated by the slope of the load displacement curve in the linear region. All mechanical tests were performed using an MTS-858 mini Bionix (MTS Systems Corp., Eden Prairie, MN) testing machine with a 500 N load cell.

Statistical Analysis

Data are expressed as the mean \pm standard deviation. Statistical analyses were performed using SPSS version 19.0

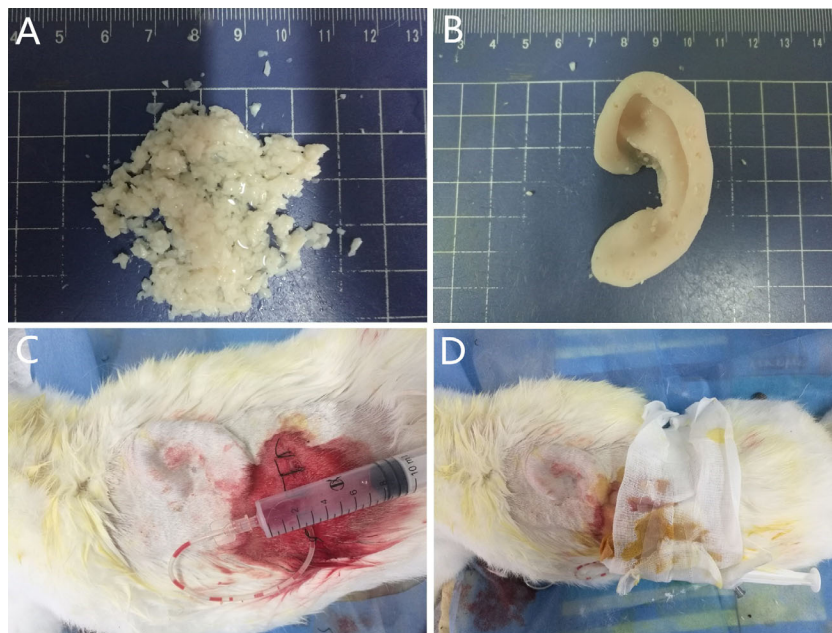


Fig. 2. Preparation of the graft and implantation in vivo. (A) Diced cartilage pieces were mixed with PRP. (B) The cartilage-PRP mix was packed into the porous, hollow auricle mold. (C) The graft was embedded into the back of the rabbit with a negative pressure drainage device. (D) Gross view of the rabbit dorsum, showing the contour of the graft under the skin and dressing. PRP = platelet-rich plasma. [Color figure can be viewed in the online issue, which is available at www.laryngoscope.com.]



Fig. 3. Gross appearance of the porous hollow auricle mold formed by 3D printing. [Color figure can be viewed in the online issue, which is available at www.laryngoscope.com.]

(IBM Corp., Armonk, NY). A Student *t* test was used to compare values, with $P < 0.05$ considered significant.

RESULTS

Gross Appearance of the Porous Hollow Auricle Mold

Porous, hollow auricle polyamide molds were printed by SLS (Fig. 3). The mold surface was smooth and contained several pores, with diameters of 0.1 to 0.3 cm. The thickness

of the mold was 0.6 mm. The internal part of the mold was hollow and completely interconnected. The base of mold was open to facilitate filling with diced cartilage. The whole mold showed good flexibility and strong mechanics.

Gross Appearance of the Auricle Shaped by Diced Cartilages

In our preliminary experiments, we found that diced cartilage pieces wrapped within a PLGA membrane were fused within 3 months.¹⁷ A greater weight of diced

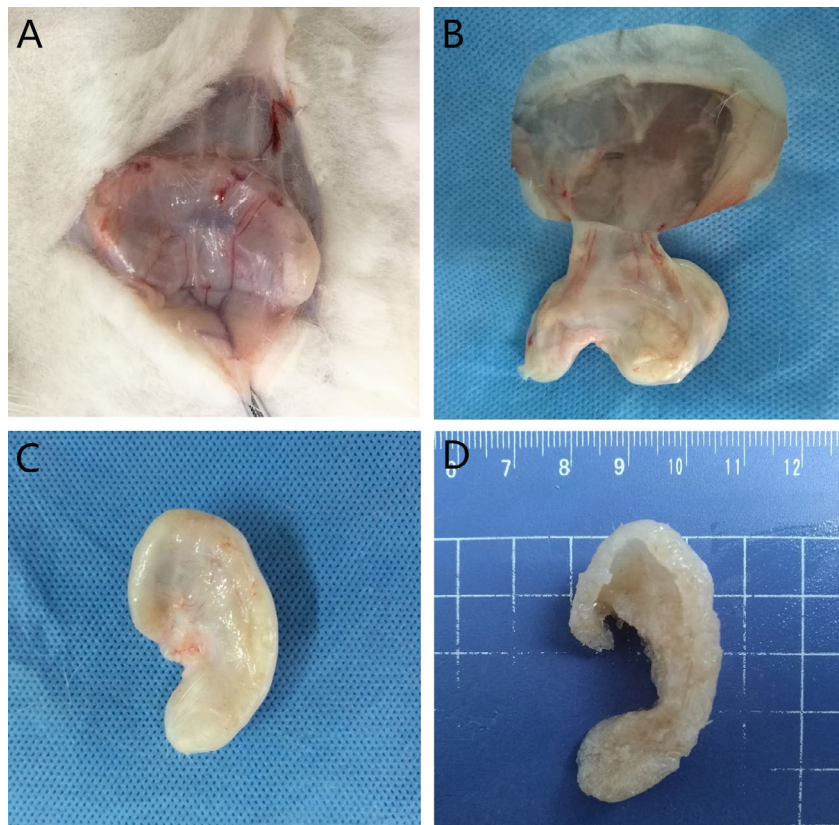


Fig. 4. The overall appearance of the auricle formed from diced cartilage mixed with PRP after 4 months. (A–B) Angiogenesis was observed from the periphery of the scaffold. (C) A fibrotic cyst had formed outside the scaffold. (D) The overall appearance of the auricle. [Color figure can be viewed in the online issue, which is available at www.laryngoscope.com.]

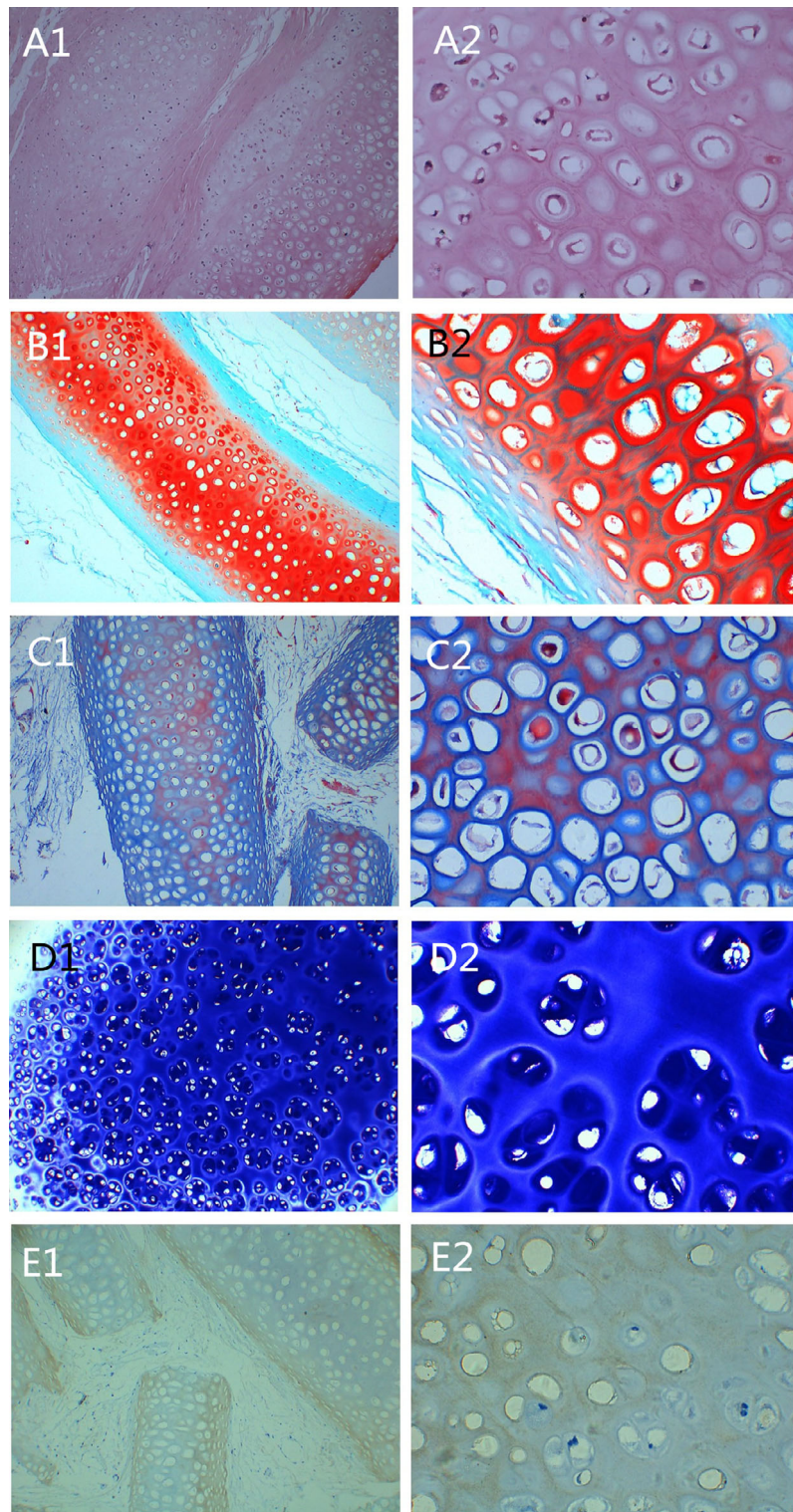


Fig. 5. Histological staining of the auricle formed from diced cartilage and platelet-rich plasma. (A1 and A2) hematoxylin and eosin staining. (B1 and B2) Safranin O staining. (C1 and C2) Masson's trichrome staining. (D1 and D2) Toluidine blue staining. (E1 and E2) type II collagen immunohistochemical staining. Left: $\times 100$; right $\times 400$. [Color figure can be viewed in the online issue, which is available at www.laryngoscope.com.]

cartilage was required to form the auricle in the present study, measuring 5.295 ± 0.327 g before transplantation. For this reason, we extended the time point of observation to 4 months.

At 4 months, the skin above the graft was incised and separated from subcutaneous tissues. A fibrotic cyst had formed around the grafts, which increased the number of peripheral vessels. There was a small amount of

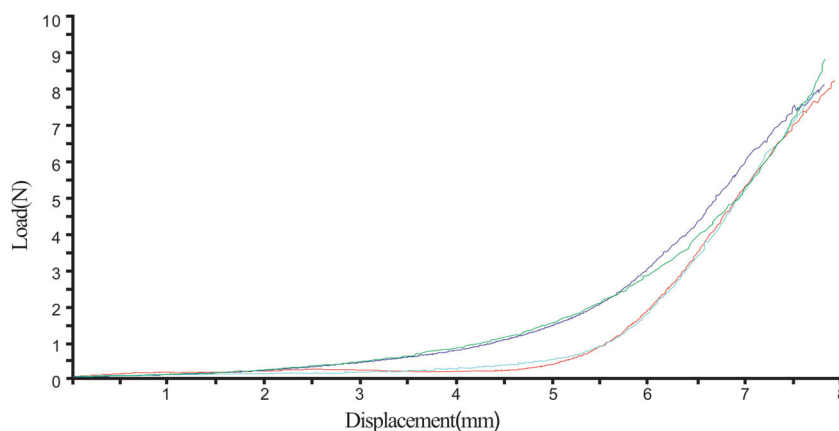


Fig. 6. Whole-ear, helix-down load displacement curve demonstrating nonlinear stiffening behavior of auricular cartilage specimens ($n = 4$). [Color figure can be viewed in the online issue, which is available at www.laryngoscope.com.]

clear organizational exudate after incision of the cyst. The whole graft was removed, and the mold was carefully cut away. The diced cartilage pieces within the mold had fused, and the gross appearance was similar in shape to an auricle. The postoperative weight was 5.157 ± 0.230 g ($P > 0.05$, compared with preoperative). Although there was evidence of incomplete fusion, most of the auricle substructures had been established, especially the outer wheel, crus of the helix, antihelix, upper and lower corner angles, and earlobe. The facies medialis of the auricle (human anatomical and physiological positions) was formed at a $\sim 25^\circ$ angle from the base, which is similar to the normal cranioauricular angle (Fig. 4).

Histological Results

Figure 5 shows HE staining of the extracellular matrix and cytoplasm of the diced cartilage as well as the presence of numerous nuclei in the cartilage lacuna, with the exception of some bright vacuoles. Fibrous tissue had grown into the spaces between the cartilage tissue. Regenerated chondroid tissue filled the peripheral areas (Fig. 5A1 and A2). In safranin O staining, numerous glycosaminoglycans (GAGs) were stained red (Fig. 5B1 and B2). In Masson's trichrome staining, cellulose fibers were red, and elastic fibers were dark blue (Fig. 5C1 and C2). In toluidine blue staining, a large amount of cartilaginous extracellular matrix was stained violet (Fig. 5D1 and D2). Type II collagen is the main type of collagen secreted by chondrocytes and plays a key role in the mechanical properties of the skeleton. To further understand the secretory function of chondrocytes and the expression of type II collagen in tissue samples, type II collagen immunohistochemical staining was performed. We observed substantial positive type II collagen staining (brown) within the extracellular matrix (Fig. 5E1 and E2). As noted above, it showed that the polyamide mold/wrapping had not interfered with the viability of diced cartilage.

Unconfined Compression Testing

In this study, the stiffness and flexibility of the newly formed auricles were evaluated by whole-ear,

helix-down compression tests; the load displacement curves are presented in Figure 6. The helix-down compression test demonstrated a mean geometric stiffness of 0.158 ± 0.187 N/mm, similar to that in humans (0.194 ± 0.202 N/mm, reported by Zopf et al.²¹).

DISCUSSION

Total reconstruction of the ear is very challenging, as evidenced by the lack of consensus among clinicians as to which technique offers the best results. The auricle has a complex 3D shape with multiple substructures. Many studies have reported preparation of auricle 3D scaffolds,^{13,18,22–24} such as gel scaffolds or biodegradable polymer scaffolds that contain chondrocytes and are filled with gold or silicone to mold the auricle shape. Although an auricle-shaped bracket could be formed in many of these cases, the distinct parts of the auricle structure were difficult to maintain and failed to achieve satisfactory aesthetics. The design of a tissue-engineered cartilage scaffold should conform to the macrostructure of tissues and organs (such as overall 3D shape) as well as the internal microstructure (including pore size, spatial distribution, pore shape, porosity, and interconnectedness) to achieve the necessary biological and mechanical performance. However, a 3D scaffold with such a balance between the internal requirements of porosity and pore size and biomechanical properties is difficult to create because porosity tends to be inversely proportional to mechanical performance.²⁵ In addition, the type of material determines the biomechanical properties of the scaffold. Nano-hydroxyapatite/polyamide 66 biomimetic composite porous scaffolds are widely used in the clinic because of their good bioactivity, mechanical properties, and bone conductivity.^{26,27} In this study, polyamide was chosen to fabricate the hollow porous mold, which satisfies the mechanical strength. The hollow nature of the mold could then be used to support the diced cartilage, which afforded the biological component and gradually united to form an appropriate auricular shape. In principle, compared with natural materials, synthetic polymer materials with low antigenicity should invoke lower immune responses, which avoids graft rejection by the

body. A preliminary experiment of the cytotoxicity of the polyamide mold showed that the material had good biocompatibility and biological safety.

Many studies have reported the difficulty in maintaining the original shape and size of tissue-engineered cartilage after transplantation. The absorption of a cartilage scaffold in vivo is caused by 1) separation from the protective perichondrium, which leads to a lack of nutritional supply; 2) variations in the mechanical environment; and 3) autoimmune and inflammatory reactions. In this study, the use of a porous, hollow mold not only provided a model for the construction of the cartilaginous graft but also offered protection for the growth of the graft, alleviating host immune intervention. Additionally, appropriate negative pressure was maintained to promote cartilage growth and fusion. Previous studies have shown that the application of a “nougat” graft—diced cartilage combined with human fibrin glue—can greatly reduce the absorption of diced cartilage in the shaping of the nasal dorsum.^{27,28} In the present study, we used PRP to enhance the viability of chondrocytes and promote the production of an appropriate extracellular matrix.¹⁷ The auricle shape remained intact, and no morphological changes were observed after the surgery.

Zopf et al. have reported that integrated, image-based, CAD, and 3D printing can be used to generate patient-specific nasal and auricular scaffolds that support cartilage regeneration.¹⁸ In principle, their designed auricular scaffold and other analogous tissue engineering scaffolds were conducive to the proliferation and shaping for chondrocytes.²⁹ However, chondrocyte activity was unavoidably influenced by some of the enzymes present in cultures in vitro. In this study, we avoided the need for cell culturing by filling our porous, hollow, auricle molds with autogenous diced cartilage.

The cartilage of the ear is elastic and comprises chondrocytes, water, GAGs, elastic fibers, and collagen fibers. In this study, the results of histological staining showed that the diced cartilages after shaping retained viable chondrocytes and a complete extracellular matrix, with positive staining for GAGs, collagen fibers, and elastic fibers, which determine the biomechanical properties of the cartilage. Many studies have reported the use of hyaline cartilage (articular, costal, and nasal septum cartilages) and fibrous cartilage (discs) in reconstructive designs; however, few have reported on the use of elastic cartilage, such as ear cartilage.²⁹ The reconstructed auricle must be able to withstand a certain degree of mechanical force to deal with the tension of the skin and daily life (e.g., sleep, wearing earplugs and helmets) but also have elasticity so as not to have potential complications later, such as extrusion through the skin. In most studies, researchers only assess the shape and size of the reconstructed auricle and tend to focus less on its biomechanical properties. In addition, there is little research on the mechanical properties of fused diced cartilage grafts. Zopf and Nimeskern performed mechanical tests on the normal ear and the subunits of ear cartilage. They found that human normal ear cartilage exhibits a nonlinear elastic material behavior similar to the mechanical behaviors of other soft tissues.^{21,30} In this study, the whole diced

cartilage-shaped auricle was examined using an unrestricted compression test. The results of load-displacement curves showed that the stiffness of the auricle (slope of the linear phase of curve) was 0.158 ± 0.187 N/mm, which is similar to that of normal human ear.²¹

In this work, the synthetic, nonbiodegradable polyamide induced a cystic-like reaction around the implant. It is unclear whether this translates in the clinical setting to the formation of a seroma or a chronic granuloma/foreign body reaction. Another limitation of this work is that we did not explore the possibility of using other biodegradable materials, such as PLGA for the hollow auricle mold.

CONCLUSION

In this study, we constructed a porous, hollow, polyamide auricular mold prepared by 3D printing technology and packed with diced cartilages and PRP. The graft showed appropriate biomechanical properties and maintained its shape, with good chondrocyte viability and the production of a cartilaginous extracellular matrix.

BIBLIOGRAPHY

1. Brent B. Auricular repair with autogenous rib cartilage grafts: two decades of experience with 600 cases. *Plast Reconstr Surg* 1992;90:355–374.
2. Nagata S. A new method of total reconstruction of the auricle for microtia. *Plast Reconstr Surg* 1993;92:187–201.
3. Romo T, Fozo MS, Sclafani AP. Microtia reconstruction using a porous polyethylene framework. *Facial Plast Surg* 2000;16:15–22.
4. Wilkes GH, Wong J, Guilfoyle R. Microtia reconstruction. *Plast Reconstr Surg* 2014;134:464e–479e.
5. Cabin JA, Bassiri-Tehrani M, Sclafani AP, Romo T. Microtia reconstruction: autologous rib and alloplast techniques *Facial Plast Surg Clin North Am* 2014;22:623–638.
6. Chauhan DS, Guruprasad Y. Auricular reconstruction of congenital microtia using autogenous costal cartilage: report of 27 cases. *J Maxillofac Oral Surg* 2012;11:47–52.
7. Berens AM, Newman S, Bhrary AD, Murakami C, Sie KC, Zopf DA. Computer-aided design and 3D printing to produce a costal cartilage model for simulation of auricular reconstruction. *Otolaryngol Head Neck Surg* 2016;155:356–359.
8. Bichara DA, O’Sullivan NA, Pomerantseva I, et al. The tissue-engineered auricle: past, present, and future. *Tissue Eng Part B Rev* 2012;18:51–61.
9. Kim YS, Yun IS, Chung S. Salvage of ear framework exposure in total auricular reconstruction. *Ann Plast Surg* 2017;78:178–183.
10. Nayyer L, Patel KH, Esmaeili A, et al. Tissue engineering: revolution and challenge in auricular cartilage reconstruction. *Plast Reconstr Surg* 2012;129:1123–1137.
11. Zhou L, Pomerantseva I, Bassett EK, et al. Engineering ear constructs with a composite scaffold to maintain dimensions. *Tissue Eng Part A*. 2011;17:1573–1581.
12. Zhang L, He A, Yin Z, et al. Regeneration of human-ear-shaped cartilage by co-culturing human microtia chondrocytes with BMSCs. *Biomaterials* 2014;35:4878–4887.
13. Shieh S, Terada S, Vacanti JP. Tissue engineering auricular reconstruction: in vitro and in vivo studies. *Biomaterials* 2004;25:1545–1557.
14. Isogai N, Morotomi T, Hayakawa S, et al. Combined chondrocyte-copolymer implantation with slow release of basic fibroblast growth factor for tissue engineering an auricular cartilage construct. *J Biomed Mater Res A*. 2005;74:408–418.
15. Erol OO. Injection of compressed diced cartilage in the correction of secondary and primary rhinoplasty: a new technique with 12 years’ experience. *Plast Reconstr Surg* 2017;140:673e–685e.
16. Liao JL, Chen J, Xu JQ, et al. Viability and biomechanics of bare diced cartilage grafts in experimental study. *J Craniofac Surg* 2017;28:1445–1450.
17. Liao JL, Chen J, He B, et al. Viability and biomechanics of diced cartilage blended with platelet-rich plasma and wrapped with poly (lactic-co-glycolic) acid membrane. *J Craniofac Surg* 2017;28:1418–1424.
18. Zopf DA, Mitsak AG, Flanagan CL, Wheeler M, Green GE, Hollister SJ. Computer aided-designed, 3-dimensionally printed porous tissue bioscaffolds for craniofacial soft tissue reconstruction. *Otolaryngol Head Neck Surg* 2015;152:57–62.
19. Liao JL, Wang SH, Chen J, Xie HJ, Zhou JD. [Progress in application of 3D bioprinting in cartilage regeneration and reconstruction for tissue engineering.] *Zhong Nan Da Xue Xue Bao Yi Xue Ban* 2017;42:221–225.

20. Sonnleitner D, Huemer P, Sullivan DY. A simplified technique for producing platelet rich plasma and platelet concentrate for intraoral bone grafting techniques: a technical note. *Int J Oral Maxillofac Implants* 2000;15: 879–882.
21. Zopf DA, Flanagan CL, Nasser HB, et al. Biomechanical evaluation of human and porcine auricular cartilage. *Laryngoscope* 2015;125:e262–e268.
22. Isogai N, Asamura S, Higashi T, et al. Tissue engineering of an auricular cartilage model utilizing cultured chondrocyte-poly (L-lactide-epsilon-caprolactone) scaffolds. *Tissue Eng* 2004;10:673–687.
23. Xu JW, Johnson TS, Motarjem PM, Peretti GM, Randolph MA, Yaremchuk MJ. Tissue-engineered flexible ear-shaped cartilage. *Plast Reconstr Surg* 2005;115:1633–1641.
24. Kamil SH, Vacanti MP, Aminuddin BS, Jackson MJ, Vacanti CA, Eavey RD. Tissue engineering of a human sized and shaped auricle using a mold. *Laryngoscope* 2004;114:867–870.
25. Huttmacher DW. Scaffolds in tissue engineering bone and cartilage. *Biomaterials* 2000;21:2529–2543.
26. Wang HN, Li YB, Zuo Y, Li J, Ma S, Cheng L. Biocompatibility and osteogenesis of biomimetic nano-hydroxyapatite/polyamide composite scaffolds for bone tissue engineering. *Biomaterials* 2007;28: 3338–3348.
27. Bracaglia R, Tambasco D, D'Ettoire M, Gentileschi S. "Nougat graft": diced cartilage graft plus human fibrin glue for contouring and shaping of the nasal dorsum. *Plast Reconstr Surg* 2012;130:741e–743e.
28. Guler I, Billur D, Aydin S, Kocaturk S. Efficacy of platelet-rich fibrin matrix on viability of diced cartilage grafts in a rabbit model. *Laryngoscope* 2015; 125:e104–e111.
29. Reiffel AJ, Kafka C, Hernandez KA, et al. High-fidelity tissue engineering of patient specific auricles for reconstruction of pediatric microtia and other auricular deformities. *PLoS One* 2013;8:e56506.
30. Nimeskern L, Pleumeekers MM, Pawson DJ, et al. Mechanical and biochemical mapping of human auricular cartilage for reliable assessment of tissue-engineered constructs. *J Biomech* 2015;48: 1721–1729.